Photodiagnosis and Photodynamic Therapy 27 (2019) 442–448

Contents lists available at ScienceDirect

Photodiagnosis and Photodynamic Therapy

journal homepage: www.elsevier.com/locate/pdpdt

The capability of nonlinear optical characteristics as a predictor for cellular uptake of nanoparticles and cell damage

Ali Abbasian Ardakani[a,b], Alireza Ghader[a,b], Hamid Asgari[a], Marzieh Keshavarz[c], Fatemeh Ebrahimi Tazehmahalleh[d], Mohammad Hosein Majles Ara[e], Malekeh Malekzadeh[b], Habib Ghaznavi[f,*], Ali Shakeri-Zadeh[a,b,*]

[a] Finetech in Medicine Research Center, Iran University of Medical Sciences (IUMS), Tehran, Iran
[b] Medical Physics Department, School of Medicine, Iran University of Medical Sciences (IUMS), Tehran, Iran
[c] Department of Medical Physics, School of Medicine, Shiraz University of Medical Sciences, Tehran, Iran
[d] University Hospital Cologne, Cologne, Germany
[e] Department of Physics, Biophotonics Lab, Applied Science Research Center (ASRC), Kharazmi University, Karaj, Iran
[f] Zahedan University of Medical Sciences (ZaUMS), Zahedan, Iran

ARTICLE INFO

Keywords:
Nanotechnology
Cell damage
Z-Scan
Nonlinear optical characteristics
Refractive index

ABSTRACT

Current methods for determining the cellular effects of a treatment modality need expensive materials and much time to provide a researcher with results. The aim of this study was to evaluate the potential of nonlinear optical characteristics of cancer cells using Z-scan technique to monitor the level of cellular uptake and cell damage caused by a nanotechnology based treatment modality. Two nanocomplexes were synthesized and characterized. The first one was made of alginate hydrogel co-loaded with cisplatin and gold nanoparticles (AuNPs) named as ACA nanocomplex. The second one, named as AA nanocomplex, was the same as ACA, but without cisplatin and this AA nanocomplex was considered as the control for ACA. Different groups of CT26 mouse colon cancer cell line received various treatments of cisplatin, ACA, and AA nanocomplexes and then the samples were prepared for Z-scan studies. The MTT assay was used to evaluate the cytotoxicity induced by different treatment modalities. Transmission electron microscopy (TEM) and inductively coupled plasma-mass spectrometry (ICP-MS) were used for qualitative and quantitative assessments of the level of AuNPs cellular uptake. The trend of nonlinear optical properties changes for treated cells was in agreement with MTT, TEM and ICP-MS results. Z-scan technique was able to successfully indicate the occurrence of cell damage. It was also capable to determine the intensity of cell damage induced by ACA nanocomplex in comparison to free cisplatin. Furthermore, Z-scan results showed that it was able to discriminate the differences of optical properties of the cells incubated with ACA nanocomplex for various incubation times. Nonlinear optical characteristics of a cell may be considered as a reliable indicator to predict the level of cellular effects induced by a nanotechnology based treatment modality. The protocol suggested in this article does not waste materials, not take much time to provide the results, and it is inexpensive technique.

1. Introduction

Although chemotherapy is one of the major treatment methods for various cancers, it suffers from serious side effects [1]. Conventional chemotherapy techniques cannot completely deliver drug to the specific cancerous tissue [2]. The dawn of nanotechnology and multifunctional nanoparticles, such as gold nanoparticles (AuNPs), made great promises to develop several proper and efficient approaches in the context of drug delivery. The advantages of using nanoparticles as drug carriers are their high stability, high biological half-life, reduced side effects of non-specific drug distribution in healthy tissues and the ability of drug administration in various ways, such as oral or *i.v.* injection. We have recently introduced a new multifunctional theranostic nanocomplex made of Alginate-Cisplatin-AuNPs, named as ACA nanocomplex [3,4]. When a new compound is generated and introduced to the field of cancer nanotechnology, it is important to determine its effects on cell proliferation or its cytotoxic effects [5]. While various cell viability assay methods are being utilized [6,7], it is important to detect what happened to the cells following the incubation of new synthesized compound with the cells as quick as possible. In addition to speed, a

* Corresponding authors at: Iran University of Medical Sciences (IUMS), Hemmat Exp., Tehran, Iran.
E-mail addresses: dr.ghaznavi@zaums.ac.ir (H. Ghaznavi), shakeriz@iums.ac.ir (A. Shakeri-Zadeh).

https://doi.org/10.1016/j.pdpdt.2019.07.023
Received 15 April 2019; Received in revised form 21 July 2019; Accepted 26 July 2019
Available online 27 July 2019

high-performance and low-cost technique is desirable. Tetrazolium reduction, resazurin reduction, protease markers, and ATP detection are some well-known examples of viability assay methods used to estimate the number of viable cells following a given treatment with a new compound [8]. These assay methods usually help us with quantification of different markers of viable cells such as some items related to cell metabolism or enzymatic activities of a viable cell [8]. Moreover, in these assay methods, we need to incubate a substance with a population of viable cells. Following such an incubation, a chemical reaction takes several hours to be completed and a colored or fluorescent product is generated. The colored or fluorescent product, which is the origin of a signal proportional to the number of viable cells, can be easily identified. Finally, the generated optical density can be simply measured using a plate reader. Colorimetric methods for viable cell measurement are considered as the high-performance modalities, but they impose cost and need much time to provide the results. As a result, it is desirable to introduce and develop a non-invasive and inexpensive method to assess the biological effects of a new treatment modality.

In various fields of biomedicine, nonlinear optical methods have recently attracted the attentions of investigators. For example, Salman et al. recently used Z-scan technique to make differentiation between benign and malignant oral tissues [9]{Salman, 2016 #844}. Also, they applied Z-scan technique to differentiate normal and carcinogenic ovarian cells [10]. We recently introduced a protocol for differentiating various tumor cell lines using Z-scan technique [11]. In addition, there are many publications reporting Z-scan as a useful technique to measure the oxidative stress of plasma lipoproteins, cholesterol, triglycerides, protein, albumin, glucose and creatinine [12]. In practice, the interaction of laser with samples is the principal section of such a proposed optical diagnostic technique [13–15].

Considering the potentials of Z-scan technique and the need for a rapid, non-invasive and inexpensive method to assess the biological effects of a new synthesized compound, we hypothesized Z-scan technique can be probably appropriate in this area. In the other words, here, we demonstrate the potentials of nonlinear optical characteristics of cancer cells determined using Z-scan technique to monitor the level of cellular uptake and cell damages after treatment by a new nanocomplex. In this regard, nonlinear refractive index of cancer cells was measured before and after various treatment modalities and its correlation with MTT assay (as a test to identify cell viability) was studied. Also, nonlinear refractive index of the cells treated with nanocomplex was investigated to find its correlation with the results of TEM and ICP-MS (as the methods for evaluating cell uptake). Fig. 1 demonstrates the present study at a glance.

2. Materials and methods

2.1. Materials

ACA nanocomplex was prepared as reported previously [3,4]. Hydrogen tetrachloroaurate (III) trihydrate, cisplatin and sodium alginate were purchased from Sigma-Aldrich (St. Louis, MO, USA) for nanocomplex synthesis. For in vitro experiments we purchased fetal bovine serum (FBS) from Gibco® (USA), RPMI-1640 cell culture medium, penicillin-streptomycin, MTT (3-[4, 5-dimethylthiazol-2-y1]-2, 5-diphenyltetrazolium bromide), and trypsin-ethylene diamine tetra acetic acid (EDTA) from the Sigma-Aldrich Company (St. Louis, MO, USA).

2.2. Characterization of ACA nanocomplex

To determine the size and morphology of the synthesized ACA nanocomplex, transmission electron microscopy (TEM; LEO906-ZEISS) was carried out. The Malvern Zetasizer Nano ZS-90 instrument was used to determine the hydrodynamic diameter and zeta potential of ACA nanocomplex. Finally, the absorption spectrum of ACA nanocomplex were analyzed using the Rayleigh UV-1601 instrument.

2.3. Cell culture and cytotoxicity assay

CT26 cell line, originated from mouse colon adenocarcinoma [16], were prepared from the Pasteur institute (Tehran, Iran) and cultured in RPMI-1640 cell culture medium supplemented with 1% penicillin -streptomycin and 10% FBS at 37 °C in an atmosphere of 5% CO_2 incubator. Cells were sub-cultured using trypsin-EDTA. Cytotoxicity of the synthesized ACA nanocomplex was evaluated using MTT assay. The protocol of MTT assay was the same as what we reported in our previous publications [3,4].

2.4. Cellular uptake assay

Investigation of nanocomplex cell uptake was done using two different methods; inductively coupled plasma mass spectrometry (ICP-MS) and transmission electron microscopy (TEM). The CT26 cells were cultured in two wells of 6-well plate (300,000 cells/well). After 24 h, the nanocomplex was incubated with the adhered cells for 12 and 24 h. Then, the cells were washed with PBS, collected using trypsin, and finally centrifuged. In this step, for each incubation time group, two separate cell pellets were obtained. One of the cell pellets was dissolved in aqua regia and examined for the Au content by ICP-MS (ELAN DRC-e spectrometer; PerkinElmer SCIEX, Concord, Ontario, Canada). Another sample of cell pellet was fixed with glutaraldehyde fixative and was examined by TEM to visualize the presence of nanocomplex inside the cells.

2.5. Optical method

The nonlinear refraction is calculated by applying the Z-scan method. The value and sign of the nonlinear refraction are given by the technique as shown in the Fig. 2. In this study, Nd:YAG Q-switched laser operating at 532 nm wavelength, with the pulse width of 100 ns and the repetition rate of 400 kHz, was used. Also, a lens was used with an 80 mm focal length. The sample is passed along the Z-axis and transmittance intensity is measured by movement. The nonlinear refraction is computed as follows [4,17]:

$$n_2 = (\lambda\, \Delta T_{P-V}) / (2\pi\, L_{eff}\, (0.406)\, (1 - S)^{0.25}\, I_0) \quad (1)$$

λ, I_0, S and L_{eff} are the laser wavelength, the maximum intensity at the focus, the fraction of beam transmitted by the aperture and effective length, respectively. These parameters are assessed in the below equations:

$$I_0 = (2P)/(\pi\, (W_0)^2) \quad (2)$$

where W_0 and P are the beam waist and the input power, respectively.

$$S = 1 - \exp\,(-2(r_a/W_a)^2) \quad (3)$$

where W_a and r_a are the beam radius and the aperture radius at the plane of the aperture, respectively.

$$L_{eff} = (1 - e^{-\alpha L})/\alpha \quad (4)$$

where L and α stand for the sample thickness and the linear absorption coefficient, respectively.

ΔT_{P-V} stands for the difference between the peak and valley ($T_P - T_V$) in the normalized diagram. The normalized transmittance graph of a sample with a positive nonlinear refraction reaches a valley at first and then increases to a peak. As opposed to that if sample has a negative nonlinear refraction, the graph is reversed.

2.6. The studied groups

Seven different groups of CT26 cells were considered in this study and then the results were obtained using the assessment methods mentioned above (MTT assay and Z-scan technique). The groups were

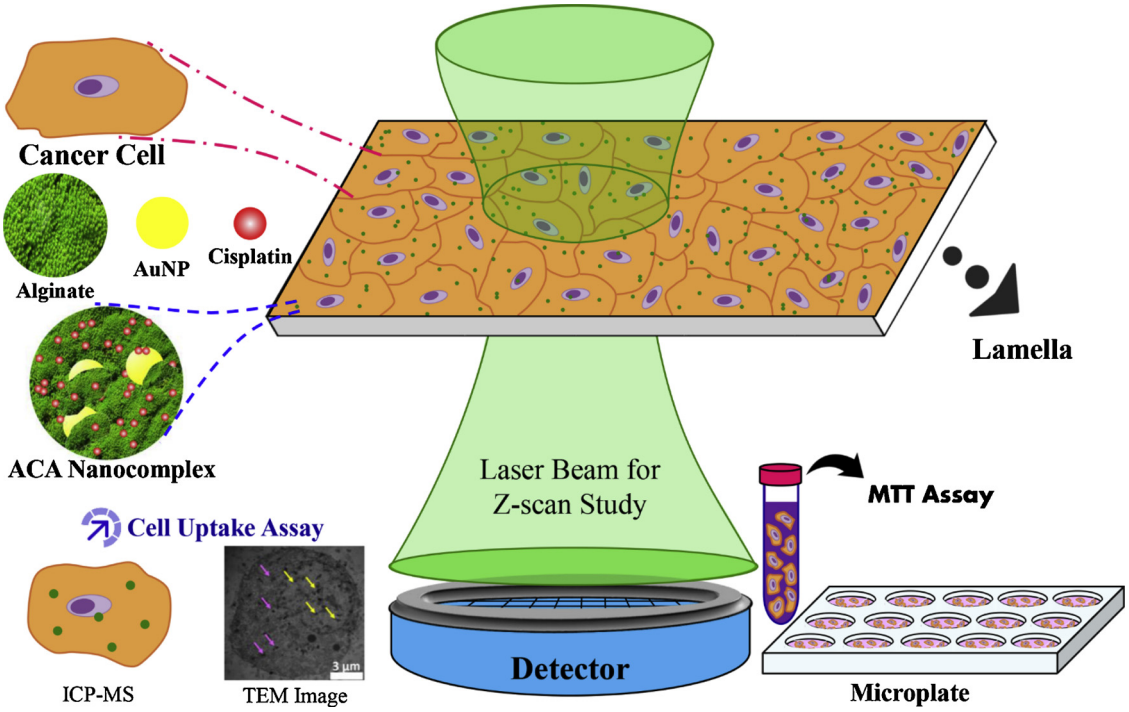

Fig. 1. The schematic illustration to show different steps of the present study at a glance.

as follows:

1 Control (the cells received no treatment)
2 CT26 cells incubated with cisplatin for 12 h
3 CT26 cells incubated with cisplatin for 24 h
4 CT26 cells incubated with ACA nanocomplex for 12 h
5 CT26 cells incubated with ACA nanocomplex for 24 h
6 CT26 cells incubated with cisplatin-free nanocomplex (AA nanocomplex) for 12 h
7 CT26 cells incubated with cisplatin-free nanocomplex (AA nanocomplex) for 24 h

2.7. Statistical analysis

One-way ANOVA test was selected for statistical analysis and it was performed using SPSS software (version 11). Tukey test at 95% confidence level was considered as a post hoc test. P-value of less than 0.05 was considered to be statistically significant. Linear regression analysis was used to measure R-squared (R^2) correlation coefficient and to assess the linearity between n_2 and cell viability following a given treatment. The R^2 coefficient is ranged from 0 to 1. The R^2 gets closer to 1 as the correlation between n_2 and cell viability is stronger.

3. Results

3.1. Characterization of ACA nanocomplex

The TEM images of the nanocomplex are shown in Fig. 3(a) wherein AuNPs can be seen as a black sphere, which are coated by alginate hydrogel appeared as the gray shell around AuNP (arrows indicate alginate coating). The hydrodynamic size distribution of ACA nanocomplex is shown in Fig. 3(b). Accordingly, it was found the effective hydrodynamic size of the nanocomplex was around 44 nm (20–80 nm range). The Zeta potential of ACA nanocomplex was obtained -35.1 mV that proves the good stability of the nanocomplex. Fig. 3(c) also shows the UV–vis spectrum of ACA nanocomplex, showing the absorption peak at 530 nm.

3.2. Cellular uptake

As stated before, we measured the level cell uptake for ACA nanocomplex using two different methods; TEM and ICP-MS analyses. TEM images presented in Fig. 4 indicated the presence of ACA nanocomplex inside the CT26 cell nucleus (yellow arrows) and cytoplasm (pink arrows). ICP-MS test also confirmed the entrance of nanocomplex into the CT26 cells by reporting the amount of Au content. We observed that 0.21 ng Au was entered into each cell following the incubation of nanocomplex with CT26 cells for 12 h. This is while we obtained higher

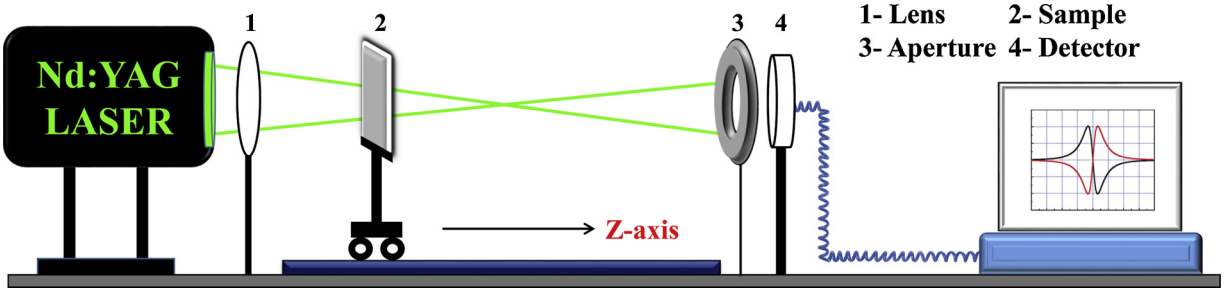

Fig. 2. Experimental setup for Z-scan technique.

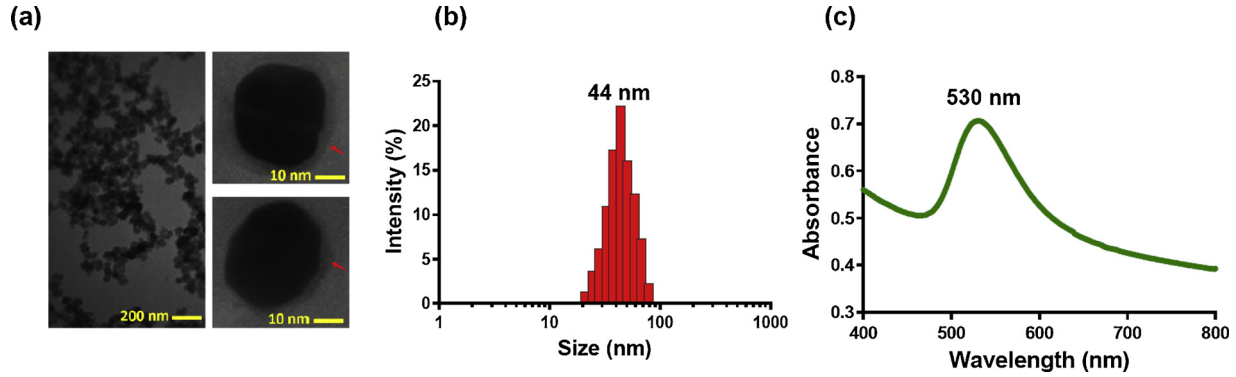

Fig. 3. Characterization of ACA nanocomplex. (a) TEM images, (b) size distribution profile, and (c) UV–vis spectrum of ACA nanocomplex (with permission from Elsevier [4]).

amount of Au in CT26 cells incubated with nanocomplex for 24 h (0.53 ng/cell).

3.3. Nonlinear optical behavior of samples

Curves of the normalized transmittance versus movement were drawn for all samples obtained from each treatment group. Fig. 5 illustrates nonlinear refraction of samples for different conditions. The maximum value of ΔT_{P-V} among the samples with negative nonlinear refraction belongs to control sample. The amount of ΔT_{P-V} decreases by incubating cells with cisplatin. Hence, the magnitude ΔT_{P-V} of incubated cells with cisplatin for 12 h is higher than 24 h.

Incubating the cells with AA nanocomplex could change the nonlinear refraction sing from negative to positive (Control vs. 12 h vs. 24 h incubation time: -7.40 vs. 2.52 vs. 5.50). It was found that ACA nanocomplex increased the magnitude of nonlinear refraction of cells compared to the AA nanocomplex for both 12 and 24 h incubation times. Table 1 presents the results of our optical experiments in details.

3.4. The results of cytotoxicity assay

MTT assay was used to evaluate the cytotoxic effects of different treatments considered in the groups listed in Section 2.6. As seen in Fig. 6, the highest level of cytotoxic effects (or the lowest level of cell viability) was seen for ACA nanocomplex at both incubation times (12 and 24 h). In comparison to the results seen for free cisplatin group (Fig. 6), at a given incubation time, ACA nanocomplex caused more cell death ($p < 0.05$). We also found a significant relation between the cell death level and incubation time for both ACA nanocomplex and cisplatin groups. When the incubation time increased from 12 h to 24 h, the cell viability was decreased from 76% to 66% and from 47% to 30% in cisplatin and ACA nanocomplex groups, respectively.

3.5. Correlation of n_2 and cell viability

Fig. 6 represents the observed correlation between n_2 and cell viability for all treatment groups. The linear regression analysis yielded a significant and high linearity for proposed optical method. In addition, the slope of plot indicates that there is negative linear relation between n_2 and cell viability ($y = 17.66 - 0.28x$).

4. Discussion

The results of the present study indicated that optical characteristics of a treated cell can be a good candidate as an endpoint to determine the cell changes induced by a given treatment modality. By analyzing the trends of changes occurred in the nonlinear refraction index of the cells in different treatment groups, it was found that the suggested optical analysis was in agreement with viability assay tests such as MTT assay. Accordingly, it may be stated that Z-scan technique has a high potential to predict the occurrence of cell damage following a given treatment modality.

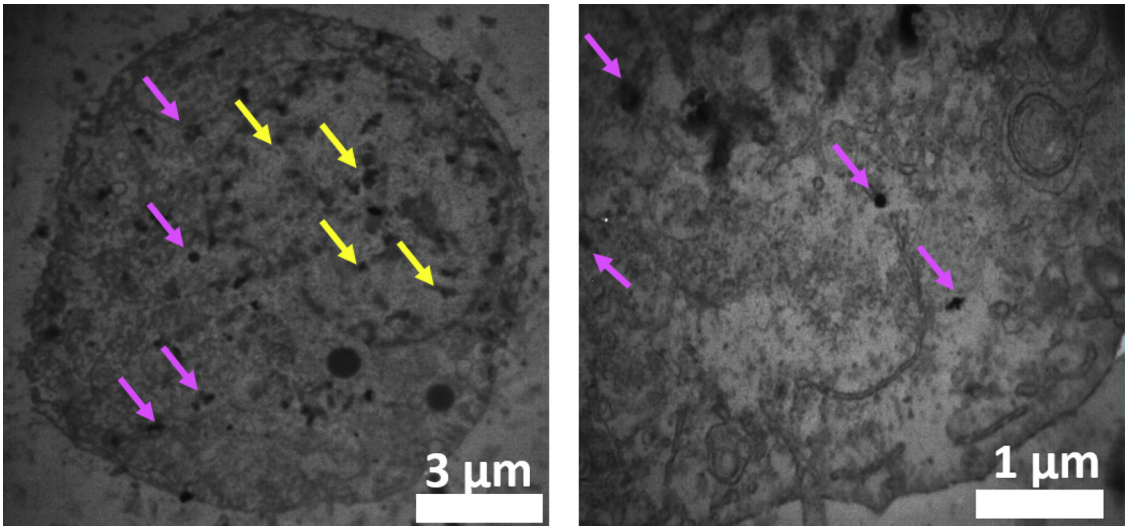

Fig. 4. TEM images of CT26 cells after incubation with ACA nanocomplex. Yellow arrows show the presence of nanocomplex in CT26 cell nucleus and the pink ones show the presence of nanocomplex inside the cytoplasm of CT26 cell.

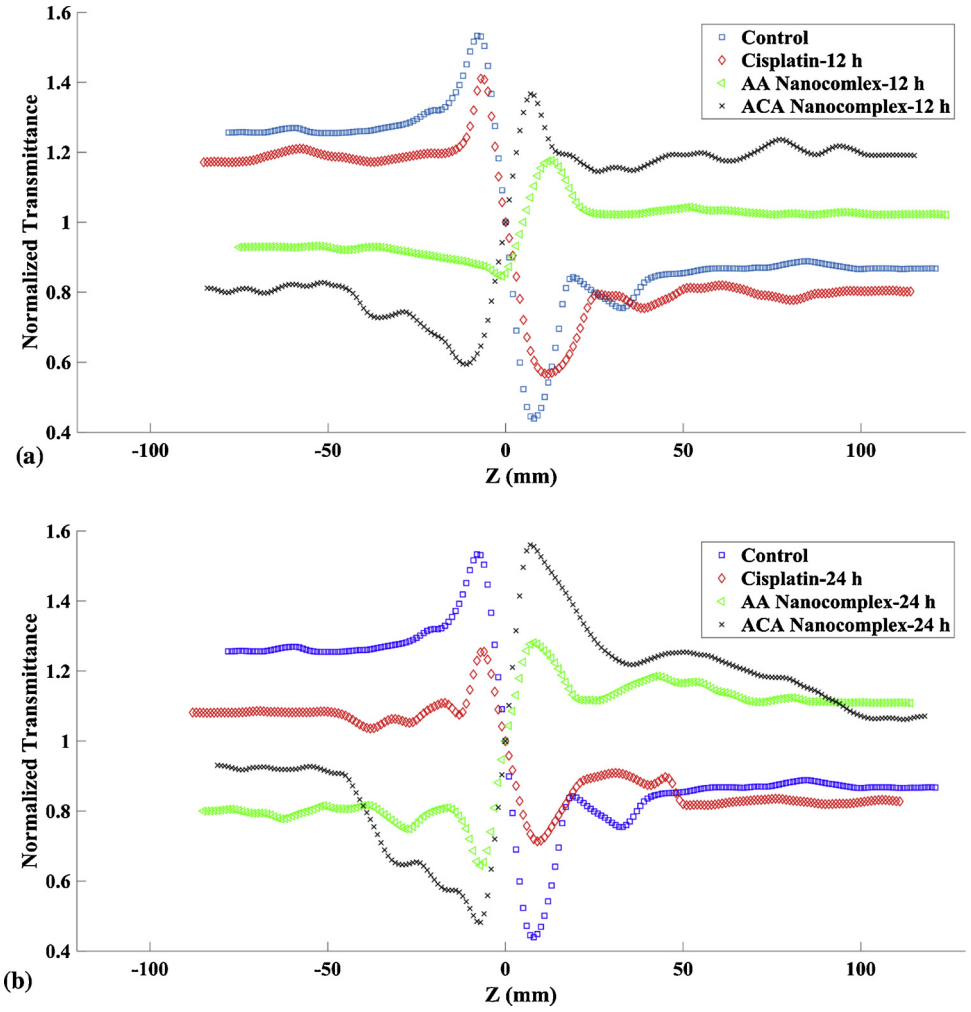

Fig. 5. Closed aperture Z-scan normalized data of (a) 12 h and (b) 24 h incubation time samples.

Table 1
Values of nonlinear refractive index for 12 h and 24 h samples.

Groups	Nonlinear Refractive Index ($n_2 \times 10^{-7}$ cm^2/w ± Error)	
	Incubation Time	
	12 h	24 h
Control	−7.40 ± 0.44	−7.40 ± 0.44
Cisplatin	−5.86 ± 0.35	−3.67 ± 0.22
AA Nanocomplex	+2.52 ± 0.15	+5.50 ± 0.33
ACA Nanocomplex	+7.11 ± 0.43	+10.89 ± 0.65

By looking at Table 1, it is found that the control cells had negative nonlinear refraction index. As the control sample cell was moved in the direction of the focal point, it did behave like a negative lens and hence made the beam parallel. Due to the smaller spot size at the aperture, a higher transmittance has been occurred across the aperture. In practice and theory, the maximum intensity occurs when the control sample is in front of the focal point. Also, the minimum intensity occurs as the control sample is passed through the focal point. As a result, a peak is seen in Fig. 5 at first and then a valley is appeared for the control sample cell. On the other hand, cisplatin induced a significant cell death (as seen in Fig. 6) and it also caused an increase in the nonlinear refractive index of treated cells (see Table 1). Cell damage after a chemotherapy regimen may be manifested through autophagy activation process, degenerating the constituents of cell nucleus, swelling

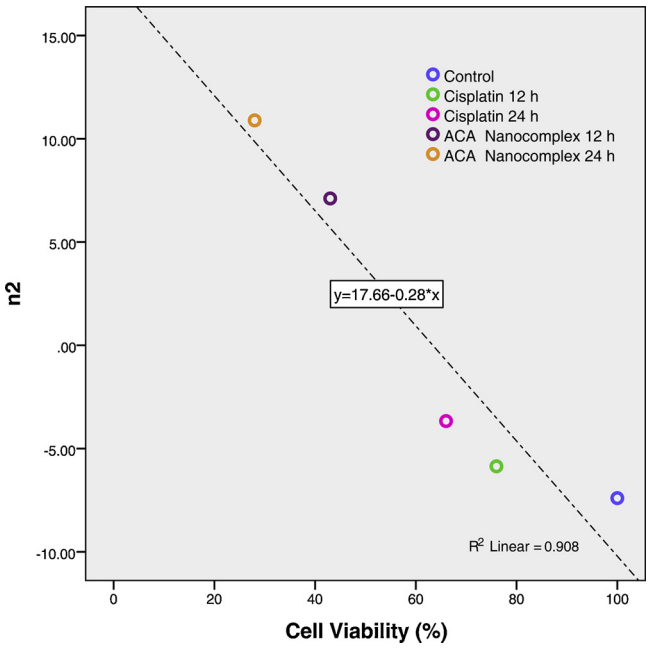

Fig. 6. Values of non-linear refractive index and CT26 cells viability following different treatments. Linear regression showed strong linearity between the results of Z-scan technique and MTT assay (R^2 = 0.908).

endoplasmic reticulum and mitochondria [18–23]. Such phenomena may degrade cell organelles and increase cytoplasmic nano-bodies and vacuoles. The main reason for changes in the optical property of a cell is related to the interaction of laser beam with cell components. In fact, scattering cross-section may increase with appearance of nano-bodies in the cell [24]. Hence, by passing laser beam through the treated cell, the scattering cross-section is increased and the cellular nano-bodies behave as a positive lens. Consequently, these events may be the reasons for the observed valley followed by a peak (Fig. 5). Actually, the cells treated with a chemotherapy drug such as cisplatin may act as a positive lens and causes an increase in the value of nonlinear refraction index.

The results also show that the sign of nonlinear refractive index is changed from negative to positive when the cells treated with AA nanocomplex. It is supposed that the AA nanocomplex can also increase the scattering cross-section, behave as a positive lens, and finally alter the nonlinear refraction index as reported in Table 1. Hence, the AA nanocomplex is responsible for changing the sign of the nonlinear refractive index of samples from negative to positive. Since the cell uptake of nanocomplex was increased with increasing the incubation time (according to the ICP-MS results), the laser beam scattering for 24 h samples was occurred more than 12 h samples. Thereby, as the incubation time increased, the value of nonlinear refraction became larger ($n_{2,12\ h}$ vs. $n_{2,24\ h}$ of AA nanocomplex: 2.52 vs. 5.50). Hence, the change in sign of n_2 may be considered as a criterion to verify the occurrence of cellular uptake.

Recent studies demonstrated that drug delivery using an efficient nano-carrier can promote and enhance the effects of traditional chemotherapy modalities. This is mainly because of increasing the chance of drug entrance into the cancer cells [25–28]. Our TEM and ICP-MS studies results indicated that ACA nanocomplex were efficiently internalized into the CT26 cells and subsequently induced greater cell death compared to free cisplatin. Moreover, higher cell death was observed for 24 h samples compared to 12 h samples. By looking at the ICP-MS results, we can find a direct relation between cellular uptake and incubation time and the resultant cell death. Again, in this section of our study, we observed that the results of Z-scan technique was in agreement with MTT assay results. There was a similar trend for changes occurred in nonlinear refraction index and MTT assay result obtained for the cells treated by ACA nanocomplex. The changes observed for nonlinear refraction index are mainly originated from existence of nanocomplex in treated cells and the resultant cell damages. To evaluate the level of cell damages induced by ACA nanocomplex, we should eliminate the effect of AA nanocomplex (as the nano-carrier of cisplatin) in optical experiments. Thereby, the nonlinear refraction of cells after incubation with AA nanocomplex was firstly measured as the control for ACA nanocomplex group. The differences obtained for AA and ACA nanocomplex treatment groups may belong to significant cell damage induced by cisplatin. As expected, incubation time can also cause more cellular damage and more changes in n_2 ($\Delta n_{2,12\ h}$ of cisplatin alone vs. ACA nanocomplex: 1.54 vs. 4.59; $\Delta n_{2,24\ h}$ of cisplatin alone vs. ACA nanocomplex: 3.73 vs. 5.39). Also, the obtained results indicated that our proposed optical method has a good linearity with cell viability tests such as MTT assay. We can conclude that the value of n_2 increases when the cell viability is decreased. Therefore, n_2 has negative correlation with cell viability or positive correlation with cell damage (see Fig. 6). These all confirm that n_2 can be used as a potential indicator to determine if a cancer cell is damaged following a given treatment.

5. Conclusion

In this article, we examined the capabilities of Z-scan as an optical approach to detect subtle cell changes after a nanotechnology based treatment modality in a non-invasive, rapid, and inexpensive manner. The results indicated that nonlinear refraction index of the cells is a reliable indicator to: (i) monitor and detect the induced cell damages following a given treatment modality and (ii) evaluate the occurrence of cellular uptake of a newly synthesized nanocomplex. Such an optical method does not waste materials, not take much time to provide the results, and it is an inexpensive technique. The main cost of this optical diagnostic method only relates to the laser set up.

Declaration of Competing Interest

Nothing to be declared.

Acknowledgements

All supports received from the Ministry of Health & Medical Education (MOHME) of Iran are acknowledged. This study was also supported by Zahedan University of Medical Sciences (grant number 7970).

References

[1] V. Lorusso, Management of chemotherapy-induced nausea and vomiting by risk profile: role of netupitant/palonosetron, Ther. Clin. Risk Manag. 12 (2016) 917–925.
[2] X. Zhai, L. Yang, S. Chen, Q. Zheng, Z. Wang, Impact of age on adjuvant chemotherapy after radical resection in patients with non-small cell lung cancer, Cancer Med. 5 (9) (2016) 2286–2293.
[3] M. Keshavarz, K. Moloudi, R. Paydar, Z. Abed, J. Beik, H. Ghaznavi, A. Shakeri-Zadeh, Alginate hydrogel co-loaded with cisplatin and gold nanoparticles for computed tomography image-guided chemotherapy, J. Biomater. Appl. 33 (2) (2018) 161–169.
[4] Z. Alamzadeh, J. Beik, V.P. Mahabadi, A.A. Ardakani, A. Ghader, S.K. Kamrava, A.S. Dezfuli, H. Ghaznavi, A. Shakeri-Zadeh, Ultrastructural and optical characteristics of cancer cells treated by a nanotechnology based chemo-photothermal therapy method, J. Photochem. Photobiol., B 192 (2019) 19–25.
[5] A. Shakeri-Zadeh, H. Eshghi, G. Mansoori, A. Hashemian, Gold nanoparticles conjugated with folic acid using mercaptohexanol as the linker, J. Nanotechnol. Prog. Int. 1 (2009) 13–23.
[6] R. Alizadeh, Z. Bagher, S.K. Kamrava, M. Falah, H.G. Hamidabadi, M.E. Boroujeni, F. Mohammadi, S. Khodaverdi, A. Zare-Sadeghi, A. Olya, Differentiation of human mesenchymal stem cells (MSC) to dopaminergic neurons: a comparison between wharton's jelly and olfactory mucosa as sources of MSCs, J. Chem. Neuroanat. 96 (2019) 126–133.
[7] N.P. Coussens, G.S. Sittampalam, R. Guha, K. Brimacombe, A. Grossman, T.D. Chung, J.R. Weidner, T. Riss, O.J. Trask, D. Auld, Assay guidance manual: quantitative biology and pharmacology in preclinical drug discovery, Clin. Transl. Sci. 11 (5) (2018) 461–470.
[8] J.L. Chen, T.W. Steele, D.C. Stuckey, Metabolic reduction of resazurin; Location within the cell for cytotoxicity assays, Biotechnol. Bioeng. 115 (2) (2018) 351–358.
[9] M. Salman, M.A.M. Hossein, K.S. Kamran, M. Shayan, Optical discrimination of benign and malignant oral tissue using Z-scan technique, Photodiagn. Photodyn. Ther. 16 (Supplement C) (2016) 54–59.
[10] M. Salman, M.A.M. Hosein, N. Mohammad, Nonlinear optical investigation of normal ovarian cells of animal and cancerous ovarian cells of human in-vitro, Optik Int. J. Light Electron Optics 127 (8) (2016) 3867–3870.
[11] A. Ghader, A.A. Ardakani, H. Ghaznavi, A. Shakeri-Zadeh, S.E. Minaei, S. Mohajer, M.H.M. Ara, Evaluation of nonlinear optical differences between breast cancer cell lines SK-BR-3 And MCF-7; An in vitro study, Photodiagn. Photodyn. Ther. 23 (2018) 171–175.
[12] S. Alves, D. Sonego, K. Fudimura, M. Hallack, L. Azzalis, V. Junqueira, K. Rocha, R. Fonseca, F. Figueiredo, F. Fonseca, The use of Z-scan technique for determination of biochemical parameters in children with solid tumors or leukemias supplemented or not with selenium, Photodiagn. Photodyn. Ther. 26 (2019) 36–42.
[13] I. Bigio, S. Bown, Spectroscopic sensing of cancer and cancer therapy: current status of translational research, Cancer Biol. Ther. 3 (3) (2004) 259–267.
[14] J.Q. Lu, K. Dong, X.-H. Hu, Effects of rough interfaces on a converging laser beam propagating in a skin tissue phantom, optical biopsy III, Int. Soc. Opt. Photonics (2000) 176–184.
[15] J. Mourant, M. Canpolat, C. Brocker, O. Esponda-Ramos, T. Johnson, A. Matanock, K. Stetter, J. Freyer, Light scattering from cells: the contribution of the nucleus and the effects of proliferative status, BIOMEDO 5 (2) (2000) 131–137.
[16] J. Beik, M.B. Shiran, Z. Abed, I. Shiri, A. Ghadimi-Daresajini, F. Farkhondeh, H. Ghaznavi, A. Shakeri-Zadeh, Gold nanoparticle-induced sonosensitization enhances the antitumor activity of ultrasound in colon tumor-bearing mice, Med. Phys. 45 (9) (2018) 4306–4314.
[17] M. Sheik-Bahae, A. Said, E.S. Van, High-sensitivity, single-beam n (2) measurements, Opt. Lett. 14 (17) (1989) 955–957.
[18] J. Lin, Y. Lin, T. Tsai, H. Chen, K. Chou, T. Hwang, Cisplatin induces protective autophagy through activation of BECN1 in human bladder cancer cells, drug design, Dev. Ther. 11 (2017) 1517–1533.
[19] R.X. Zhang, L.Y. Li, J. Li, Z. Xu, A.Z. Abbasi, L. Lin, M.A. Amini, W.Y. Weng, Y. Sun,

A.M. Rauth, Coordinating biointeraction and bioreaction of a nanocarrier material and an anticancer drug to overcome membrane rigidity and target mitochondria in multidrug-resistant cancer cells, Adv. Funct. Mater. 27 (39) (2017) 1700804.
[20] B. Arya, S. Mittal, P. Joshi, A. Pandey, J. Ramirez-Vick, S. Singh, Graphene oxide-chloroquine nanoconjugate induce necroptotic death in A549 cancer cells through autophagy modulation, Nanomedicine (London, England) 13 (18) (2018) 2261–2282.
[21] S. Hu, X. Li, R. Xu, L. Ye, H. Kong, X. Zeng, H. Wang, W. Xie, The synergistic effect of resveratrol in combination with cisplatin on apoptosis via modulating autophagy in A549 cells, Acta Biochim. Biophy. Sin. 48 (6) (2016) 528–535.
[22] B. Ahmed, S. Dwivedi, M. Abdin, A. Azam, M. Al-Shaeri, M. Khan, Q. Saquib, A. Al-Khedhairy, J. Musarrat, Mitochondrial and chromosomal damage induced by oxidative stress in Zn2+ ions, ZnO-bulk and ZnO-NPs treated Allium cepa roots, Sci. Rep. 7 (2017) 40685.
[23] X. Zhang, M. Zhang, Q. Cong, M. Zhang, M. Zhang, Y. Lu, C. Xu, Hexokinase 2 confers resistance to cisplatin in ovarian cancer cells by enhancing cisplatin-induced autophagy, Int. J. Biochem. Cell Biol. 95 (2018) 9–16.
[24] A. Cox, A.J. DeWeerd, J. Linden, An experiment to measure mie and Rayleigh total scattering cross sections, Am. J. Phys 70 (6) (2002) 620–625.
[25] W. Song, L. Shen, Y. Wang, Q. Liu, T. Goodwin, J. Li, O. Dorosheva, T. Liu, R. Liu, L. Huang, Synergistic and low adverse effect cancer immunotherapy by immunogenic chemotherapy and locally expressed PD-L1 trap, Nat. Commun. 9 (1) (2018) 2237.
[26] J. Xi, L. Da, C. Yang, R. Chen, L. Gao, L. Fan, J. Han, Mn2+-coordinated PDA@DOX/PLGA nanoparticles as a smart theranostic agent for synergistic chemo-photothermal tumor therapy, Int. J. Nanomed. 12 (2017) 3331–3345.
[27] L. Tan, R. Huang, X. Li, S. Liu, Y. Shen, Controllable release of nitric oxide and doxorubicin from engineered nanospheres for synergistic tumor therapy, Acta Biomater. 57 (2017) 498–510.
[28] J. Lee, J. Kim, Y. Lee, D. Park, S. Im, E. Song, H. Park, W. Kim, Self-assembled nanocomplex between polymerized phenylboronic acid and doxorubicin for efficient tumor-targeted chemotherapy, Acta Pharmacol. Sin. 38 (6) (2017) 848–858.